

[Click here to view linked References](#)

High noise correlation between the functionally connected neurons in emergent V1 microcircuits.

Vishal Bharmauria^{1,2}, Lyes Bachatene^{1,2}, Sarah Cattan^{1,2}, Nayan Chauria^{1,2}, Jean Rouat^{1,2,3}, Stéphane Molotchnikoff^{1,2,3}

¹ Neurophysiology of Visual System, Université de Montréal, Département de Sciences Biologiques, Montréal, Qc, Canada

² Neurosciences Computationnelles et Traitement Intelligent des Signaux (NECOTIS), Sherbrooke, Qc, Canada

³ Département de Génie Électrique et Génie Informatique, Université de Sherbrooke, Sherbrooke, Qc, Canada

*Correspondence: Dr S. Molotchnikoff, Université de Montréal, Sciences Biologiques CP 6128 Succ. centre-ville Montréal, Quebec H3C 3J7 CANADA

E-mail: stephane.molotchnikoff@umontreal.ca +1 514 343 6616

Acknowledgments

SM and JR were supported by CRSNG (Conseil de Recherches en Sciences Naturelles et en Génie) FRQ-NT (Fonds de recherche du Québec - Nature et technologies). Grant No: NSERC, Canada 6943-1210.

Author Contributions

VB did the experiments, analyzed the data and wrote the manuscript. LB SC and NC participated in the experiments and analyses of data. JR contributed to the analyses of data. VB and SM conceived the idea of study. SM contributed to data analyses and manuscript writing.

Conflict of interest

The authors report no conflict of interest.

1
2
3
4 **Abstract**
5
6

7 Neural correlations (noise correlations and cross-correlograms) are widely studied to infer functional
8 connectivity between neurons. High noise correlations (Rsc) between neurons have been reported to
9 increase the encoding accuracy of a neuronal population; however, low noise correlations have also been
10 documented to play a critical role in cortical microcircuits. Therefore, the role of noise correlations in
11 neural encoding is highly debated. To this aim, through multi-electrodes, we recorded neuronal ensembles
12 in the primary visual cortex of anesthetized cats. By computing cross-correlograms (CCGs), we divulged
13 the functional network (microcircuit) between neurons within an ensemble in relation to a specific
14 orientation. We show that functionally connected neurons systematically exhibit higher noise correlations
15 than functionally unconnected neurons in a microcircuit that is activated in response to a particular
16 orientation. Furthermore, the mean strength of noise correlations for the connected neurons increases
17 steeply than the unconnected neurons as a function of the resolution-window used to calculate noise
18 correlations. We suggest that, neurons that display high noise correlations in emergent microcircuits feature
19 functional connections which are inevitable for information encoding in the primary visual cortex.
20
21
22
23
24
25
26
27
28
29
30
31
32

33
34 Keywords: Cell-assembly, Cross-correlation (CCG), Functional connection, Noise correlation (Rsc)
35
36

37 **Introduction**
38
39

40 There is mounting evidence that understanding of information encoding in brain requires studying the
41 correlation (noise correlation or Rsc; cross-correlations or CCG) between neurons (Perkel et al. 1967;
42 Alloway and Roy 2002; Bach and Kruger 1986; Zohary et al. 1994; Averbeck and Lee 2003; Barthó et al.
43 2004; Uhlhaas et al. 2009; Cohen and Kohn 2011; Graf et al. 2011; Cotton et al. 2013; Cossell et al. 2015).
44 Rsc is the trial-by-trial Pearson correlation of the spike counts of two neurons in response to the same
45 stimulus, and it simply gives us information about the degree to which trial-by-trial fluctuations are shared
46 by a neuron pair (Averbeck et al. 2006; Cohen and Kohn 2011). On the other hand, a 'CCG' is a histogram
47 of the firing rate of the target neuron with reference to the spiking of another neuron, and it provides the
48 direction and type of functional link between neurons (Alonso and Martinez 1998; Barthó et al. 2004;
49 Fujisawa et al. 2008; Bharmauria et al. 2014; Bharmauria et al. 2015). A peak offset from zero (quasi-
50
51
52
53
54
55
56
57
58
59
60
61
62
63
64
65

1
2
3
4 **synchrony** in a ‘CCG’ indicates a putative excitatory or inhibitory connection, whereas a peak straddling
5
6 zero (synchrony) signifies a common input to neurons (Perkel et al. 1967; Shadlen and Newsome 1998;
7
8 Dong et al. 2008; Bachatene et al. 2012).
9

10
11 On one hand, many previous studies (in the visual cortex of different species) have reported high Rsc
12
13 between neurons (Gawne et al. 1996; Kohn and Smith 2005; Gutnisky and Dragoi 2008; Cohen and Kohn
14
15 2011; Cotton et al. 2013; Cossell et al. 2015), suggesting that highly correlated neurons may share a great
16
17 deal of sensory input (Zohary et al. 1994; Shadlen and Newsome 1998; Bair et al. 2001; Kohn and Smith
18
19 2005). On the other hand, decorrelated firing (**low Rsc**) has also been observed in V1 microcircuits (Ecker
20
21 et al. 2010; **Renart etl. 2010**), implying that highly correlated variability may be detrimental to population
22
23 coding (Zohary et al. 1994; Sompolinsky et al. 2001). **Investigators have also reported in V1 that, a CCG**
24
25 **between a neuronal pair fluctuates systematically with the stimulus (orientation) irrespective of low or high**
26
27 **Rsc between them (Gawne et al. 1996; Bair et al. 2001; Reich et al. 2001; Kohn and Smith 2005).** Thus, a
28
29 contentious debate persists concerning the precise nature of Rsc in microcircuits (Cohen and Kohn 2011;
30
31 Averbeck et al. 2006)
32

33
34 A major factor while calculating Rsc is the counting window (resolution-window, as we name it) that is
35
36 employed to compute Rsc (Cohen and Kohn 2011; Hansen et al. 2012; **Schulz et al. 2015**). Shorter
37
38 windows may underestimate the true Rsc between neurons, whereas bigger windows may add artificial
39
40 correlation between spike-trains (Cohen and Kohn 2011; Hansen et al. 2012).
41

42
43 **Recently, we have shown that a salient functional network (microcircuit) is activated within an ensemble**
44
45 **(Bharmauria et al. 2015b, in press) in a characteristic 50-ms window of opportunity, wherein neurons**
46
47 **cooperate synergistically exhibiting augmented power of gamma oscillations (Bharmauria et al. 2014;**
48
49 **Bharmauria et al. 2015a).** In the current investigation, we report that, **in such an emergent microcircuit**
50
51 **framed by an ensemble** (simultaneously recorded neurons from a microelectrode), the connected pairs
52
53 exhibit significantly higher Rsc than the unconnected pairs at all the resolution-windows. **Moreover,**
54
55 **consistent with the previous findings (Gawne et al. 1996; Bair et al. 2001; Reich et al. 2001; Kohn and**
56
57 **Smith 2005), the value of Rsc between a pair is independent of the presented orientation in an ensemble**
58
59 **irrespective of the activation or inactivation of a functional connection between them at that orientation.** To
60

1
2
3
4 our knowledge, this investigation is the first to systematically investigate the connected and unconnected
5
6 pairs based on correlations (Rsc and CCG) **in a microcircuit**. This report further corroborates the earlier
7
8 finding (Cossell et al. 2015) that, high Rsc between the strongly connected neurons carries well defined and
9
10 structured information in microcircuits. However, importantly, **Rsc has** to be calculated in optimal
11
12 resolution-windows to extract meaningful information from **these microcircuits**. We suggest that highly
13
14 **correlated (stable or strong connections)** neurons are major junctions of information routing in quasi-
15
16 simultaneously active cohorts of neurons.
17

18 19 **Materials and methods**

20 21 **Ethical approval**

22
23
24 Five adult animals (Cats) were prepared for electrophysiological recordings in the primary visual cortex
25
26 (layer II/III, area 17), as per the guidelines of Canadian Council on Animal Care and approved by the
27
28 Institutional Animal Care and Use committee of Université de Montreal. The procedure is as below.
29

30 31 **Animals, anaesthesia and surgical procedures**

32
33
34 Animals premedicated with acepromazine maleate (Atravet, Wyeth-Ayerst, Guelph, ON, Canada; 1 mg/kg,
35
36 intramuscular) and atropine sulphate (ATRO-SA, Rafter, Calgary, AB, Canada; 0.04 mg/kg, intramuscular)
37
38 were anesthetized with ketamine hydrochloride (Rogarsetic, Pfizer, Kirkland, QC, Canada; 25 mg/kg,
39
40 intramuscular). The cats were then paralyzed with 40 mg and maintained with 10 mg/kg/h of gallamine
41
42 triethiodide (Flaxedil, Sigma Chemical, St. Louis, MO, USA; intravenous) administered in 5% dextrose
43
44 lactated Ringer's nutritive solution. General anesthesia was maintained by artificial ventilation with a
45
46 mixture of N₂O/O₂ (70:30) supplemented with 0.5% isoflurane (AErrane, Baxter, Toronto, ON, Canada).
47
48 Electroencephalogram, electrocardiogram, rectal temperature and end-tidal CO₂ partial pressure were
49
50 monitored throughout the experiment, and kept in physiological ranges. The pupils were dilated with
51
52 atropine sulfate (1%, Isopto-Atropine; Alcon, Mississauga, Ontario, Canada) and the nictitating membranes
53
54 were retracted with phenylephrine hydrochloride (2.5%, Mydfrin, Alcon). The loci of the area centrales
55
56 were inferred from the position of the blind spots which were ophthalmoscopically focused and projected
57
58
59
60
61
62
63
64
65

1
2
3
4 onto a translucent screen. At the end of the experiment, the cats were euthanized intravenously with a dose
5
6 (0.5 mL/kg) of Sodium Pentobarbital (CEVA, Sante Animale).
7
8

9 **Visual stimulation**

10
11 Monocular stimulation was done. The multi-unit receptive fields (RF) were mapped as the minimum
12
13 response field (Barlow et al. 1967) by using a hand-held ophthalmoscope after clearly detectable activity
14
15 had been obtained. These preliminary tests revealed qualitative properties such as dimensions, velocity-
16
17 preference, orientation, and directional selectivity of neurons. Visual stimuli were generated with a VSG
18
19 2/5 graphic board (Cambridge Research Systems, Rochester, England) and displayed on a 21-inch monitor
20
21 (Sony GDM-F520 Trinitron, Tokyo, Japan) placed 57 cm from the cat's eyes, with 1024×768 pixels,
22
23 running at 100-Hz frame refresh. The blank screen was uniformly gray (~ 35 Cd/m²). Contrast was set at
24
25 80%. Mean luminance was 40 cd/m². Optimal spatial and temporal frequencies were set at 0.24 cycles/deg
26
27 and a range of 1.0–2.0 Hz, respectively, where V1 neurons are driven maximally by sine-wave drifting
28
29 gratings (Bardy et al. 2006). The tested orientations were presented in a random order. Each drifting grating
30
31 was presented in blocks of 25 trials (each trial lasted 4.1 s) with varying inter-stimulus (1–3 s) intervals
32
33 during which no stimulus was presented (Fig. 1a). Thus the presentation of a stimulus lasted 180 s (with all
34
35 trials and inter-stimulus intervals).
36
37
38

39 **Electrophysiological recording and single-unit selection**

40
41
42 Multi-unit activity in the primary visual cortex was recorded by a tungsten multi-electrode (Frederick Haer
43
44 & Co, Matrix Electrode; the multi-electrode had four columns, and each column had one row). The
45
46 recordings were performed at locations 410 or 820 μ m apart (Fig. 1b). Twelve recordings (24 sites) were
47
48 done across all cats either in the left or the right hemisphere. Recordings were performed in the
49
50 supragranular layers (cortical depth < 1000 μ m; mean = 650 μ m). The signal from the microelectrodes was
51
52 amplified, band-pass filtered (300 Hz–3 kHz), digitized and recorded with a 0.05 ms temporal resolution
53
54 (Spike2, CED, Cambridge, England). Spike sorting from the multi-unit signals was done. Neurons were
55
56 discriminated on the basis of three criteria: 1) the spike-waveform difference 2) principal component
57
58 analysis (PCA) showing well dissociated clusters 3) and auto-correlograms (ACG) showing no events
59
60
61
62
63
64
65

1
2
3
4 (indicative of the refractory period of neuron) at the central point (Csicsvari et al. 1998; Barthó et al. 2004;
5
6 Bharmauria et al. 2014). The stability of each cell's activity across conditions was verified qualitatively by
7
8 the visual control of the disposition of clusters and the shapes of waveforms. Cluster analysis was
9
10 performed using Spike2, CED, Cambridge, England in a 3-dimensional plot. The isolation distance was
11
12 calculated as the Mahalanobis distance. The Mahalanobis distance is the distance from the cluster center
13
14 within which as many events belong to the other clusters as to the specified cluster (Harris *et al.*, 2001). In
15
16 other words, given the multivariate data values for which the values in each variable are normally
17
18 distributed around a mean, this measure allows to define boundaries of constant probability around the
19
20 multi-dimensional center of the distribution. Thus, this estimation allows the separation of a cluster from
21
22 the nearest cluster. Units within a Mahalanobis distance of 2.5 were considered for further analysis of the
23
24 spike trains to reveal the functional connections between them. An example of dissociated spikes from
25
26 multiunit activity is shown in Fig. 1c. The corresponding PCA and auto-correlograms are shown in Fig. 1d
27
28 and Fig. 1e respectively.
29

30 31 **Cross-correlogram (CCG) computation**

32
33 Cross-correlograms were computed (binwidth = 1 ms) between the neural activities of all the possible
34
35 neuron pairs at all the applied orientations to reveal the functional connections. The raw CCGs were shift-
36
37 corrected (one spike train shifted over one stimulus period) to eliminate the putative significant peaks due
38
39 to the simultaneous stimulation of both cells during each trial (to remove the stimulus-evoked and locked
40
41 components) (Perkel et al. 1967). A significant peak of 2 ms (two adjacent bins) or at least one significant
42
43 bin (Alloway & Roy, 2002) was searched within a window of ± 5 ms offset from zero (excluding the ± 1 ms
44
45 bins around zero) in the shift-corrected CCG to reveal a functional connection between two neurons. The
46
47 statistical threshold for the significant peak was set at 95%, and the probability (P) of the neuronal firing in
48
49 a bin is calculated according to Abeles (1982). The details are present in Bharmauria et al (2014).
50
51

52 53 **Calculation of noise correlation (Rsc)**

54
55 Noise correlation represents the trial-by-trial Pearson correlation-coefficient between the simultaneous
56
57 firing of two neurons in response to the presentation of an identical stimulus (Cohen and Kohn 2011). Rsc
58
59 was calculated for the connected and unconnected pairs across all **ensembles** at one selected orientation
60
61
62
63
64
65

1
2
3
4 where the most number of connections were found. An optimal or near optimal orientation was chosen for
5 closely tuned assemblies, whereas an orientation exhibiting maximum connections was selected for
6 assemblies with wide orientation spreads. Rsc was calculated over all 25 trials for a neuron pair. The
7 respective trials of the pair were correlated. The Rsc-computation was performed over three different
8 counting windows (resolution-window) separately (5 ms, 25 ms and 50 ms). A resolution-window is the
9 equally sized bin into which the whole trial duration is divided to perform the Rsc-computation. For
10 example, in our case, a trial of 4 sec yielded 800 bins when the resolution-window was set at 5 ms.
11
12
13
14
15
16
17
18

19 **Results**

20
21 The aim of the current investigation was to systematically compare the noise correlation between the
22 functionally connected (as revealed from the CCGs, see methods) and unconnected neuron pairs in V1
23 **microcircuits activated within an ensemble.** It is to be noted that, within the context of this paper,
24 simultaneously recorded neurons from a microelectrode are termed **an ensemble** (that is, coactive neurons
25 as Miller et al (2014) have defined them). **It is to be underlined that a particular microcircuit activated**
26 **within an ensemble at a specific orientation (for closely tuned ensembles an optimal or non-optimal**
27 **orientation that exhibited numerous connections was chosen, and for distantly tuned ensembles an**
28 **orientation that exhibited maximum connections was chosen) was selected to systematically compare the**
29 **connected and unconnected neurons.** Across twenty four sites, 94 neurons were recorded; 62 functionally
30 connected and 47 unconnected pairs were analysed.
31
32
33
34
35
36
37
38
39
40
41
42

43 **Revealing the functional connection between neurons**

44
45 Neurons in physical proximity share a great deal of peripheral input (Averbeck and Lee 2003; Shadlen and
46 Newsome 1998), therefore, it is expected that they exhibit abundant functional connections with each other.
47 **Previously we have shown that a 'signature' functional network is framed by an ensemble contingent upon**
48 **the presented orientation (Bharmauria et al. 2015b, in press).** **We computed CCGs to reveal these functional**
49 **connections within an ensemble.** A typical example of a connected and an unconnected neuron pair is
50 shown in Fig. 2. Fig. 2a illustrates the raster plots of two simultaneously recorded neurons with respective
51 waveforms as insets. Fig. 2b shows the CCG between the above spike trains (light green neuron is the
52 reference), and the significant (the green background indicates the significance level, see methods) peak
53
54
55
56
57
58
59
60
61
62
63
64
65

1
2
3
4 off-set from zero (within 5 ms) indicates that the reference neuron projects onto the target neuron (Barthó et
5 al. 2004; Bharmuria et al. 2015). The probability (P) of the peak that reflects the strength of connection is
6 0.016. The cumulative histogram of the target neuron (black curve above the CCG) further signifies that,
7
8 once the reference neuron fires, it leads to an upsurge in the activity of the target neuron transiently. Fig. 2c
9 illustrates the raster plots (waveforms as insets) of an unconnected pair (absence of the significant peak) as
10 inferred from the CCG (light red neuron is the reference) in Fig. 2d. It is to be noted that the above three
11 neurons (same target neuron in both cases) were recorded simultaneously from a microelectrode, thus
12 constitute an ensemble.
13
14
15
16
17
18
19
20

21 High noise correlation between the functionally connected neurons in an assembly

22
23 Recently, in mouse visual cortex, it has been shown that highly correlated (Rsc) neurons are strongly
24 connected to each other (Cossell et al. 2015). After computing CCGs that revealed the functional
25 connections, we calculated Rsc for the connected and unconnected pairs in an ensemble (at a specific
26 microcircuit) at different resolution-windows. Fig. 3 shows an example of Rsc-comparison between the
27 connected and unconnected pairs in an ensemble (four simultaneously recorded neurons). The first matrix
28 (Fig. 3a) illustrates the connectivity and the strength (colored scale) of the functional connections as
29 divulged by CCGs. Out of the six possible pairs, three pairs (red-cyan; red-blue; blue-cyan) were
30 connected, and the other three pairs were unconnected. It is to be noted that the matrix is symmetric along
31 the diagonal (that is, the same connection is also represented on other side of diagonal). Fig. 3b shows the
32 Rsc-values for the same pairs at 5-ms resolution-window (see methods). The Rsc-strength seems to be
33 almost equivalent for all pairs. However, the Rsc-values for the respective pairs increased systematically as
34 we increased the resolution-windows from 5-ms to 25-ms (Fig. 3c) to 50-ms (Fig. 3d). The strength of Rsc
35 for the connected pairs increased steeply than the unconnected pairs. Fig. 3e further shows the difference in
36 increase in Rsc for the connected (green curves) and unconnected pairs (red curves). For example, the Rsc
37 values for the blue-cyan (connected) pair increased steeply from 0.02 at 5-ms to 0.16 at 25-ms to 0.19 at
38 50-ms window; whereas for the red-purple (unconnected) pair, the respective Rsc values were found to be
39 0.00, 0.01 and 0.04. On a microcircuit basis (Fig. 3f), the mean correlation (with SD) for the connected
40 pairs increased from 0.02 ± 0.00 at 5-ms to 0.12 ± 0.03 at 25-ms to 0.14 ± 0.03 at 50-ms window; whereas,
41 the corresponding values for the unconnected pairs were found to be 0.00 ± 0.00 ; 0.00 ± 0.13 and $0.04 \pm$
42
43
44
45
46
47
48
49
50
51
52
53
54
55
56
57
58
59
60
61
62
63
64
65

1
2
3
4 0.00. Both curves were significantly different (unpaired t-test, $p < 0.05$). In summary, in a **microcircuit**
5 **activated within an ensemble**, the connected neuron pairs **systematically carry high Rsc** than the
6
7 unconnected neurons, implying that neurons **with high Rsc** may be strongly related to the presented feature.
8
9

10 **Strength of connection (P), noise correlation (Rsc) and resolution-window**

11
12 Many investigators (Zohary et al. 1994; Graf et al. 2011; Hansen et al. 2012; Cossell et al. 2015) have
13 suggested that high Rsc is directly related to the strength of the connection between neurons. We thus
14 investigated how the probability of the peak **(P)** in the CCG might be related to Rsc between the same
15 neurons. Fig. 4a depicts that there is no relation between P and Rsc when Rsc was calculated in a low (5ms)
16 resolution-window, as the regression curve did not deviate significantly from zero ($p > 0.05$). However,
17 when the similar analysis was performed at 25-ms (Fig. 4b) and 50-ms (Fig. 4c) windows, the regression
18 curves significantly deviated from zero in either case ($p < 0.05$), thus, indicating that as the Rsc value
19 increases, the peak-probability in the CCG tends to increase too. In short, this analysis points to the fact that
20 Rsc has to be calculated in optimal resolution-windows to undermine the true correlation between the firing
21 of two neurons. **In other words, in optimal resolution-windows, it is possible to associate the strength of the**
22 **connections (P) to Rsc; if Rsc is high, P is high too.**
23
24
25
26
27
28
29
30
31
32
33
34
35
36

37 **Rsc dynamics within a microcircuit in relation to the presented orientation**

38
39 **As discussed above, we have already shown that an ensemble frames a specific functional network**
40 **(microcircuit) that is strictly related to the presented orientation (Bharmauria et al. 2015b, in press). We**
41 **next examined the fluctuation of Rsc for the same neurons pairs in an ensemble (that is, from one**
42 **microcircuit to another) as the orientation tilted in 22.5° steps. An example of an ensemble comprising four**
43 **neurons (all neurons were tuned approximately to 90°) is shown in Fig. 5a. A specific network is activated**
44 **at each presented orientation. The red-blue pair remains unconnected in all networks, exhibiting almost**
45 **similar Rsc values (Fig. 5b). The red-green pair is connected at four orientations exhibiting high Rsc**
46 **values, except at 135° where it displays a low Rsc value and displaying no connection. Interestingly, in**
47 **other four pairs, neurons remained unconnected regardless of the high values of Rsc in these microcircuits.**
48 **For example, the red-orange pair exhibited highest Rsc (0.17) at 45°, but failed to display a connection.**
49 **This seems to be in line with previous reports (Gawne et al. 1996; Bair et al. 2001; Reich et al. 2001; Kohn**
50
51
52
53
54
55
56
57
58
59
60
61
62
63
64
65

1
2
3
4 and Smith 2005) wherein investigators documented that the peak in CCG was orientation-dependent,
5
6 whereas the respective Rsc of the involved neurons was independent of the tilt in orientation. Hence it
7
8 appears that Rsc and CCGs have to be appropriately associated to each other in microcircuits. With this
9
10 example and other analyses, we show that within an emergent microcircuit, the connected pairs always
11
12 exhibit higher average Rsc values than the unconnected pairs (it is to be noted that in all the microcircuits,
13
14 the connected pairs always had higher average Rsc than unconnected pairs).

17 **Significant difference between the connected and the unconnected pairs**

18
19
20 Finally, all the connected and unconnected pairs were pooled as separate groups to observe the global trend
21
22 of variation of Rsc as a function of the resolution-window (Fig. 6). The mean Rsc (with SEM) for the
23
24 connected pairs (n = 62) increased steeply from 5-ms to 25-ms to 50-ms window (0.02 ± 0.00 to $0.13 \pm$
25
26 0.01 to 0.18 ± 0.01 respectively) and significantly differed (respective values for the unconnected class
27
28 were 0.00 ± 0.00 ; 0.01 ± 0.00 and 0.04 ± 0.00) from the unconnected pairs (n = 47) at every resolution-window
29
30 (Kolmogorov-Smirnov test, $p < 0.05$). This coincides with previous reports (Hansen et al. 2012; Schulz et
31
32 al. 2015), wherein they reported that noise correlation increased with the resolution-window. In summary,
33
34 we may suggest that whenever two neurons in a "microcircuit" exhibit high Rsc, this may augur a
35
36 functional connection between them.

39 **Discussion**

40
41
42 In this study, the noise correlation (Rsc) was systematically compared for the connected and the
43
44 unconnected neuron pairs in V1 microcircuits. We found that Rsc-values were significantly higher and
45
46 different for the connected neuron pairs than the unconnected pairs. Further, we found that the peak-
47
48 probability (indicative of strength of the connection) in the CCG increases with Rsc at higher resolution-
49
50 windows.

53 **Methodological considerations**

54
55
56 The current experiments were done on anaesthetized cats and we have already shown that the disclosed
57
58 functional connections are strongly related to the presented stimulus rather than the spontaneous
59
60 fluctuations in the brain — the proportion of connections was more at stimulus conditions than at

1
2
3
4 spontaneous activity; the gamma power was high at stimulus presentation than at spontaneous oscillations
5
6 (Bharmauria et al. 2014; Bharmauria et al. 2015a, Bharmauria et al. 2015b, in press). Many investigations
7
8 have reported that nearby neurons carry high noise correlations between them (Zohary et al. 1994; Kohn
9
10 and Smith 2005; Graf et al. 2011; Cossell et al. 2015). One may also argue that high noise correlation
11
12 between the connected neurons in current investigation might be attributed to the artificial binning of spikes
13
14 in wider resolution windows, but if it were the case we would not have obtained such trendy difference
15
16 between the connected and the unconnected pairs. Moreover, Cohen and Kohn (2011) have suggested that
17
18 noise correlation between the jittered spike trains (since the peaks in CCGs that revealed the functional
19
20 connections were jittered in our case, that is, offset from zero) have to be calculated over higher resolution-
21
22 windows and longer trial durations in order to capture the full strength of Rsc. Because we used higher
23
24 resolution-windows and longer trial durations to calculate Rsc, we may infer that indeed the functionally
25
26 connected neurons carry higher noise correlation between their spike trains in emergent cortical
27
28 microcircuits.
29
30

31 **Functional consequences**

32
33
34 Recently, through calcium imaging and electrode recordings in slices of mouse V1 (Cossell et al. 2015),
35
36 investigators have shown that nearby neurons exhibiting higher spike-count correlations are strongly
37
38 connected to each other, and are predominantly responsible for feature encoding. We found that, in general,
39
40 the strength of connections increases as a function of Rsc (although in higher resolution windows) between
41
42 neurons. Thus, we may suggest that neurons with higher Rsc were strongly connected to each other and
43
44 played a major role in stimulus processing.
45
46

47
48 Along the same lines (as suggested by Cossell et al. 2015), we may also suggest that in layer II/III, majority
49
50 of the input to a strongly connected neuron (a reader neuron as postulated by Buzsáki, 2010) is provided by
51
52 other neurons that share the similar tuning property as the reader neuron. Indeed, this investigation extends
53
54 the work on ensembles (Miller et al. 2014; Reid et al. 2015; Bharmauria et al. 2015b), wherein authors have
55
56 shown that same ensembles are active in response to the stimulus and even at spontaneous oscillations. We
57
58 have already reported that a signature microcircuit is activated in such an ensemble that is strictly related to
59
60 the presented stimulus (Bharmauria et al. 2015b). Reid et al (2015) documented that within the sequential
61
62
63
64
65

1
2
3
4 activation of ensembles in a Hebbian assembly, neurons fire with repeating firing patterns in an ensemble
5
6 called ‘doublet pathways’. Such recurring patterns of spiking activity were revealed through CCGs by us
7
8 that were indicative of functional connections between neurons. Furthermore, building upon these
9
10 investigations, herein, we show that within a particular microcircuit framed by an ensemble, the connected
11
12 neurons systematically exhibit higher Rsc than the unconnected neurons. Moreover, we also report that,
13
14 Rsc between neurons is independent of the presented orientation and the neurons may or may not exhibit
15
16 connections from one orientation to another irrespective of the strength of Rsc. We suggest that the
17
18 “inherent” temporal spiking pattern between neurons confers them almost equivalent Rsc along the
19
20 presented orientations (Miller et al. 2014; Reid et al. 2015; Bharmauria et al. 2015b), but on occasions it
21
22 may not be possible to reveal it through CCGs as the firing rate varies from one orientation to another. This
23
24 study also relates to another recent study by Shimono and Beggs (2014), wherein they revealed such
25
26 functional links in small clusters (3-6 neurons) using transfer entropy. Collectively, this may imply that
27
28 every presented stimulus drives the ensemble in such a way that, a group of neurons (connected) within it
29
30 covaries its responses systematically than the group of cells (unconnected) whose firings are independent of
31
32 each other. Such strongly connected neurons feature a small proportion of connected neurons in distributed
33
34 cortical circuits, and are implicated in major processing and transformation of information along the
35
36 pathways. On the other hand, the weaker connections might be attributed to the plasticity based rules, that
37
38 is, they can change (strengthen) contingent upon the input as has already been shown by Bharmauria et al
39
40 (2015b, in press) — that a specific network between V1 neurons (layer II/III) is activated by a particular
41
42 orientation. When the orientation changes, another network might be framed within the same ensemble —
43
44 wherein, some connections may remain (strong) in relation to the previous orientation and other
45
46 connections may become active.

47
48
49 From this study, we may conclude that, high noise correlations between neurons in cortical microcircuits
50
51 augur functional interactions between them; however, it is important to calculate the noise correlation in
52
53 appropriate resolution-windows to extract meaningful information from these simultaneously active local
54
55 cohorts of neurons. This study along with our previous studies might form a premise for computational
56
57 modeling to further our understanding of neural circuits.
58
59
60
61
62
63
64
65

1
2
3
4 **References**
5
6

- 7 Abeles M (1982) Quantification, smoothing, and confidence limits for single-units' histograms. *J Neurosci*
8 *Methods* 5:317-325
9
- 10 Alonso JM, Martinez LM (1998) Functional connectivity between simple cells and complex cells in cat
11 striate cortex. *Nat Neurosci*.1:395-403.
12
- 13 Alloway KD, Roy SA (2002) Conditional cross-correlation analysis of thalamocortical neurotransmission.
14 *Behav Brain Res* 135:191-196
15
- 16 Averbeck BB, Lee D (2003) Neural noise and movement-related codes in the macaque supplementary
17 motor area. *J Neurosci* 23:7630-7641
18
- 19 Averbeck BB, Latham PE, Pouget A (2006) Neural correlations, population coding and computation. *Nat*
20 *Rev Neurosci* 7: 358-366
21
- 22 Bach M, Kruger J (1986) Correlated neuronal variability in monkey visual cortex revealed by a multi-
23 microelectrode. *Exp Brain Res* 61:451-456
24
- 25 Bachatene L, Bharmauria V, Rouat J, Molotchnikoff S (2012) Adaptation-induced plasticity and spike
26 waveforms in cat visual cortex. *Neuroreport* 23:88-92
27
- 28 Bair W, Zohary E, Newsome WT (2001) Correlated firing in macaque visual area MT: time scales and
29 relationship to behavior. *J Neurosci* 21:1676-1697
30
- 31 Bardy C, Huang JY, Wang C, FitzGibbon T, Dreher B (2006) 'Simplification' of responses of complex cells
32 in cat striate cortex: suppressive surrounds and 'feedback' inactivation. *J Physiol* 574:731-750
33
- 34 Barlow HB, Blakemore C, Pettigrew JD (1967) The neural mechanism of binocular depth discrimination. *J*
35 *Physiol* 193:327-342
36
- 37 Barthó P, Hirase H, Monconduit L, Zugaro M, Harris KD, Buzsáki G (2004) Characterization of
38 neocortical principal cells and interneurons by network interactions and extracellular features. *J*
39 *Neurophysiol* 92:600-608
40
- 41 **Bharmauria V, Bachatene L, Cattan S, Brodeur S, Chanauria N, Rouat J, Molotchnikoff S (2015b) Network**
42 **selectivity and stimulus discrimination in the primary visual cortex: cell-assembly dynamics. *Eur J***
43 ***Neurosci* (in press)**
44
- 45 Bharmauria V, Bachatene L, Cattan S, Chanauria N, Rouat J, Molotchnikoff S (2015a) Stimulus-dependent
46 augmented gamma oscillatory activity between the functionally connected cortical neurons in the
47 primary visual cortex. *Eur J Neurosci* 41:1587-1596
48
- 49 Bharmauria V, Bachatene L, Cattan S, Rouat J, Molotchnikoff S (2014) Synergistic activity between
50 primary visual neurons. *Neuroscience* 268:255-264
51
- 52 Buzsáki G (2010) Neural syntax: cell assemblies, synapsembles, and readers. *Neuron* 68:362-385
53
- 54 **Carrillo-Reid L, Miller JE, Hamm JP, Jackson J, Yuste R (2015) Endogeneous sequential cortical activity**
55 **evoked by visual stimuli. *J Neurosci* 35: 8813-8828**
56
- 57 Cohen MR, Kohn A (2011) Measuring and interpreting neuronal correlations. *Nat Neurosci* 14:811-819
58
59
60
61
62
63
64
65

- 1
2
3
4 Cossell L, Iacaruso MF, Muir DR, et al. (2015) Functional organization of excitatory synaptic strength in
5 primary visual cortex. *Nature* 518:399-403
6
- 7 Cotton RJ, Froudarakis E, Storer P, Saggau P, Tolias AS (2013) Three-dimensional mapping of
8 microcircuit correlation structure. *Front Neural Circuits* 7:151
9
- 10 Csicsvari J, Hirase H, Czurko A, Buzsáki G (1998) Reliability and state dependence of pyramidal cell-
11 interneuron synapses in the hippocampus: an ensemble approach in the behaving rat. *Neuron*
12 21:179-189
13
- 14 Denman DJ, Contreras D (2014) The structure of pairwise correlation in mouse primary visual cortex
15 reveals functional organization in the absence of an orientation map. *Cereb Cortex* 24:2707-2720
16
- 17 Dong Y, Mihalas S, Qiu F, von der Heydt R, Niebur E (2008) Synchrony and the binding problem in
18 macaque visual cortex. *J Vis* 8:1-16
19
- 20 Ecker AS, Berens P, Keliris GA, Bethge M, Logothetis NK, Tolias AS (2010) Decorrelated neuronal firing
21 in cortical microcircuits. *Science* 327:584-587
22
- 23 Fujisawa S, Amarasingham A, Harrison MT, Buzsáki G (2008) Behavior-dependent short-term assembly
24 dynamics in the medial prefrontal cortex. *Nat Neurosci* 11:823-833
25
- 26 Gawne TJ, Kjaer TW, Hertz JA, Richmond BJ (1996) Adjacent visual cortical complex cells share about
27 20% of their stimulus-related information. *Cereb Cortex* 6:482-489
28
- 29 Graf AB, Kohn A, Jazayeri M, Movshon JA (2011) Decoding the activity of neuronal populations in
30 macaque primary visual cortex. *Nat Neurosci* 14:239-245
31
- 32 Gutnisky DA, Dragoi V (2008) Adaptive coding of visual information in neural populations. *Nature*
33 452:220-224
34
- 35 Hansen BJ, Chelaru MI, Dragoi V (2012) Correlated variability in laminar cortical circuits. *Neuron* 76:590-
36 602
37
- 38 Harris KD, Hirase H, Leinekugel X, Henze DA, Buzsáki G (2001) Temporal interaction between single
39 spikes and complex spike bursts in hippocampal pyramidal cells. *Neuron* 32:141-149
40
- 41 Kohn A, Smith MA (2005) Stimulus dependence of neuronal correlation in primary visual cortex of the
42 macaque. *J Neurosci* 25:3661-3673
43
- 44 Miller JE, Ayzenshtat I, Carrillo-Reid L, Yuste R (2014) Visual stimuli recruit intrinsically generated
45 cortical ensembles. *Proc Natl Acad Sci USA*, 111:E4053-4061.
46
- 47 Perkel DH, Gerstein GL, Moore GP (1967) Neuronal spike trains and stochastic point processes. I. The
48 single spike train. *Biophys J* 7:391-418
49
- 50 Reich DS, Mechler F, Victor JD (2001) Independent and redundant information in nearby cortical circuits.
51 *Science* 294: 2566-2568
52
- 53 Schulz DP, Sahani M, Carandini M (2015) Five key factors determining pairwise correlations in visual
54 cortex. *J Neurophysiol* 114:1022-1033
55
- 56 Shadlen MN, Newsome WT (1998) The variable discharge of cortical neurons: implications for
57 connectivity, computation, and information coding. *J Neurosci* 18:3870-3896
58
59
60
61
62
63
64
65

1
2
3
4 Shimono M, Beggs JM (2014) Functional clusters, hubs, and communities in the cortical microconnectome.
5 Cereb Cortex 25: 3743-3757
6

7 Sompolinsky H, Yoon H, Kang K, Shamir M (2001) Population coding in neuronal systems with correlated
8 noise. Phys Rev E Stat Nonlin Soft Matter Phys 64:051904
9

10 Swindale NV (1998) Orientation tuning curves: empirical description and estimation of parameters. Biol
11 Cybern 78:45-56
12

13 Uhlhaas PJ, Pipa G, Lima B, Melloni L, Neunenschwander S, Nikolić D, Singer W (2009) Neural synchrony
14 in cortical networks: history, concept and current status. Front Integr Neurosci 3:17
15

16 Zohary E, Shadlen MN, Newsome WT (1994) Correlated neuronal discharge rate and its implications for
17 psychophysical performance. Nature 370:140-143
18
19
20

21 Legends

22
23 **Fig. 1** A schematic of the experiment (a) Presentation of sine-wave drifting gratings in a random fashion.
24 (b) Multi-unit recording in layer II/III (area 17) in the primary visual cortex. (c) An example of four
25 neurons sorted from multi-unit activity recorded from a microelectrode. Each neuron has a distinct
26 waveform and a well dissociated cluster. (d) Corresponding auto-correlograms (ACGs) for the isolated
27 neurons.
28

29
30 **Fig. 2** Inferring functional connectivity (a) Respective raster plots and perievent histograms of two
31 simultaneously recorded neurons (waveforms as insets) from a microelectrode. (b) The cross-correlogram
32 (CCG) between the spike trains of neurons (light green neuron is the reference) yielded a significant peak
33 ($P = 0.016$) offset from zero (blue broken line), thus indicating that the reference neuron projects onto the
34 target neuron. (c) Respective responses of two simultaneously recorded neurons (waveforms as insets) that
35 did not exhibit a functional connection between them, as revealed from the non-significant CCG in (d).
36 Note: The target neuron is same in both cases.
37
38

39 **Fig. 3** High noise correlation between functionally connected neurons in a microcircuit (a) Functional
40 connectivity matrix between four simultaneously recorded neurons from a microelectrode. Neurons along
41 the x-axis project onto the y-axis neurons. Note: the matrix is symmetric along the diagonal, that is, the
42 same connection is also represented on the other side of the diagonal. The colored scale stands for the
43 strength of the connection. (b,c,d) Rsc- matrices of the same neurons at 5-ms, 25-ms and 50-ms resolution-
44 windows respectively. The colored scale in 'b' stands for all the matrices. (e) Noise-correlation as a
45 function of the resolution-window for each pair in the microcircuit. The green curves represent the
46 connected neuron pairs and the red lines correspond to the unconnected pairs. (f) Mean noise correlation
47 for connected and unconnected neuron pairs as a function of the resolution window. The mean correlation is
48 higher and significantly different for the connected pairs than the unconnected pairs (unpaired t-test, $p <$
49 0.05)
50
51

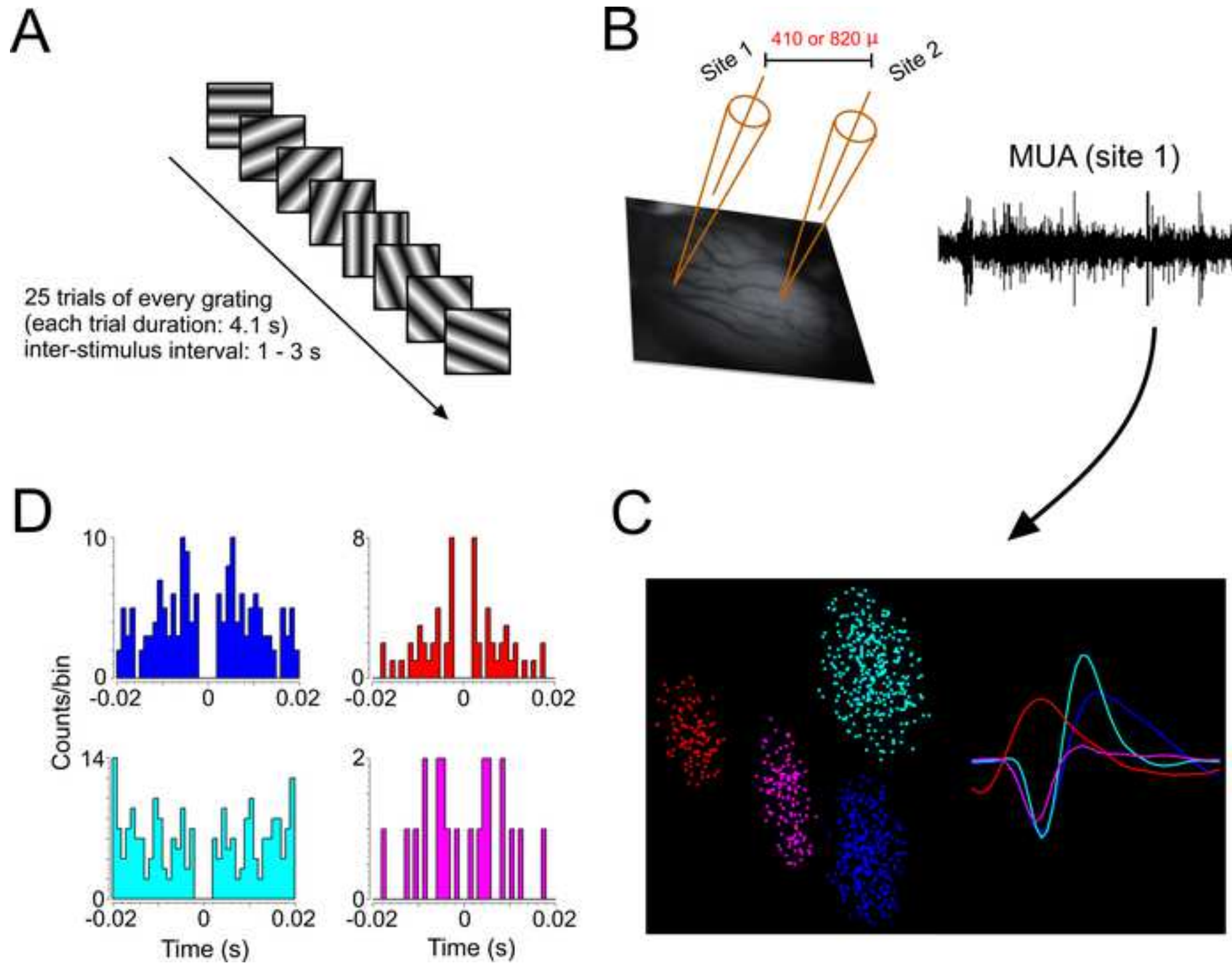
52
53 **Fig. 4** Peak-probability (P), noise correlation (Rsc) and the resolution-window. (a) No relation is inferred
54 between P and Rsc at 5-ms resolution-window as the regression curve did not deviate significantly from
55 zero ($p > 0.05$). (b,c) 'P' and Rsc in relation to the 25-ms and 50-ms resolution windows. 'P' showed a
56 significant relation with Rsc at both resolution windows ($p < 0.05$).
57

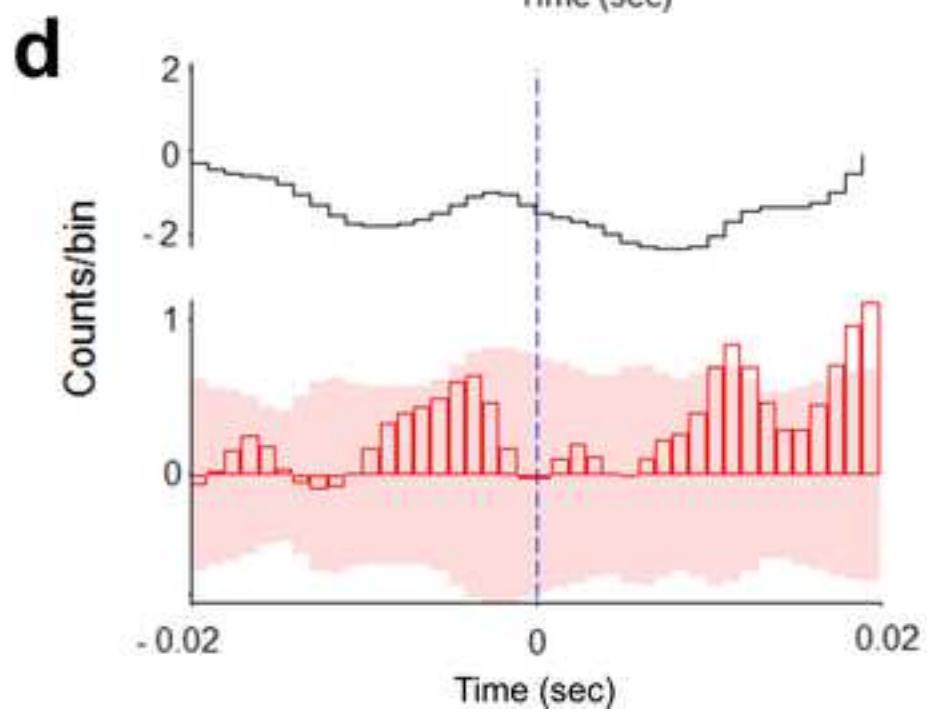
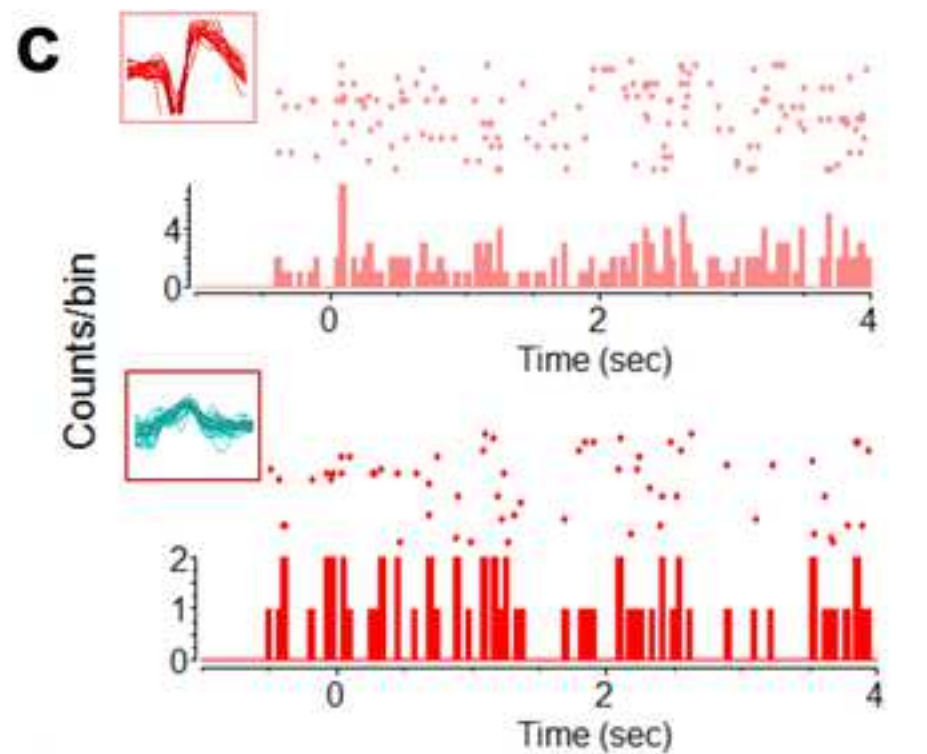
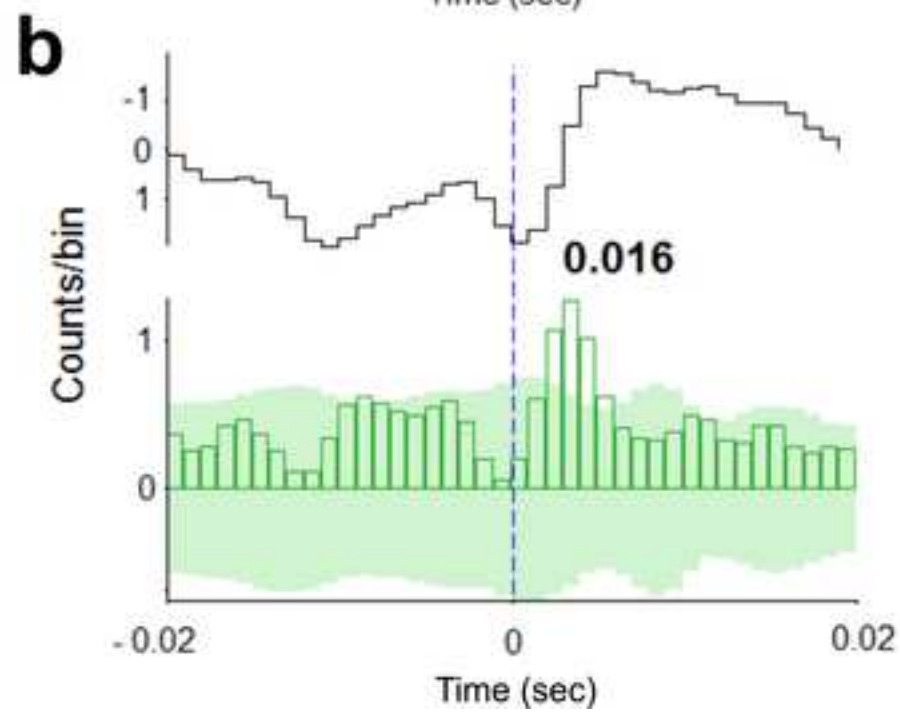
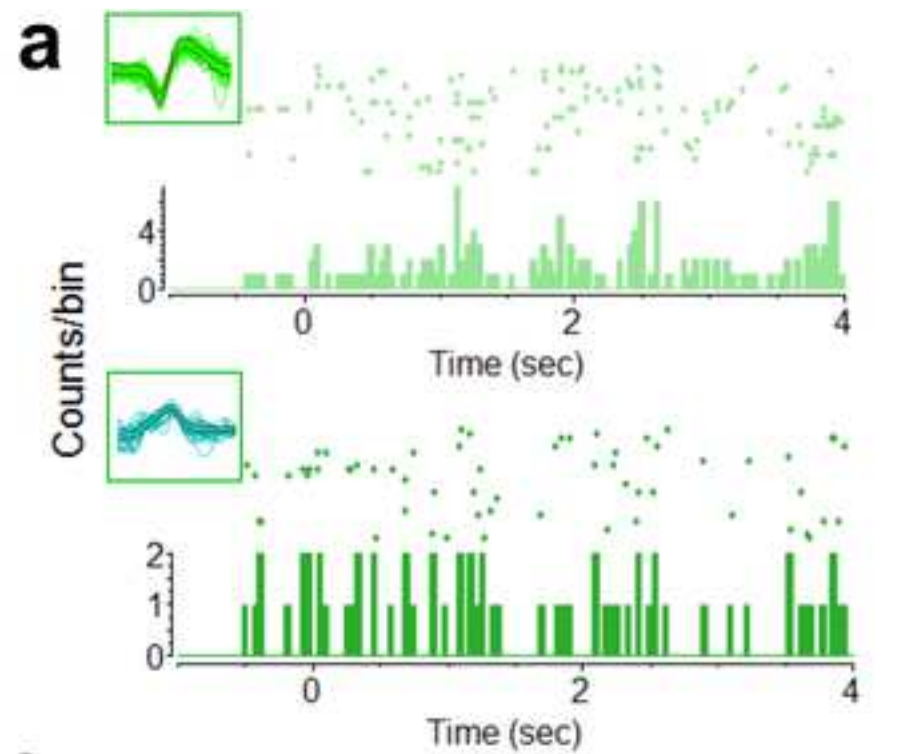
58 **Fig. 5** An example of the dynamics of Rsc in an ensemble in relation to the presented orientation. (a)
59 Activation of an emergent microcircuit contingent upon the presented orientation within an ensemble. (b)
60
61
62
63
64
65

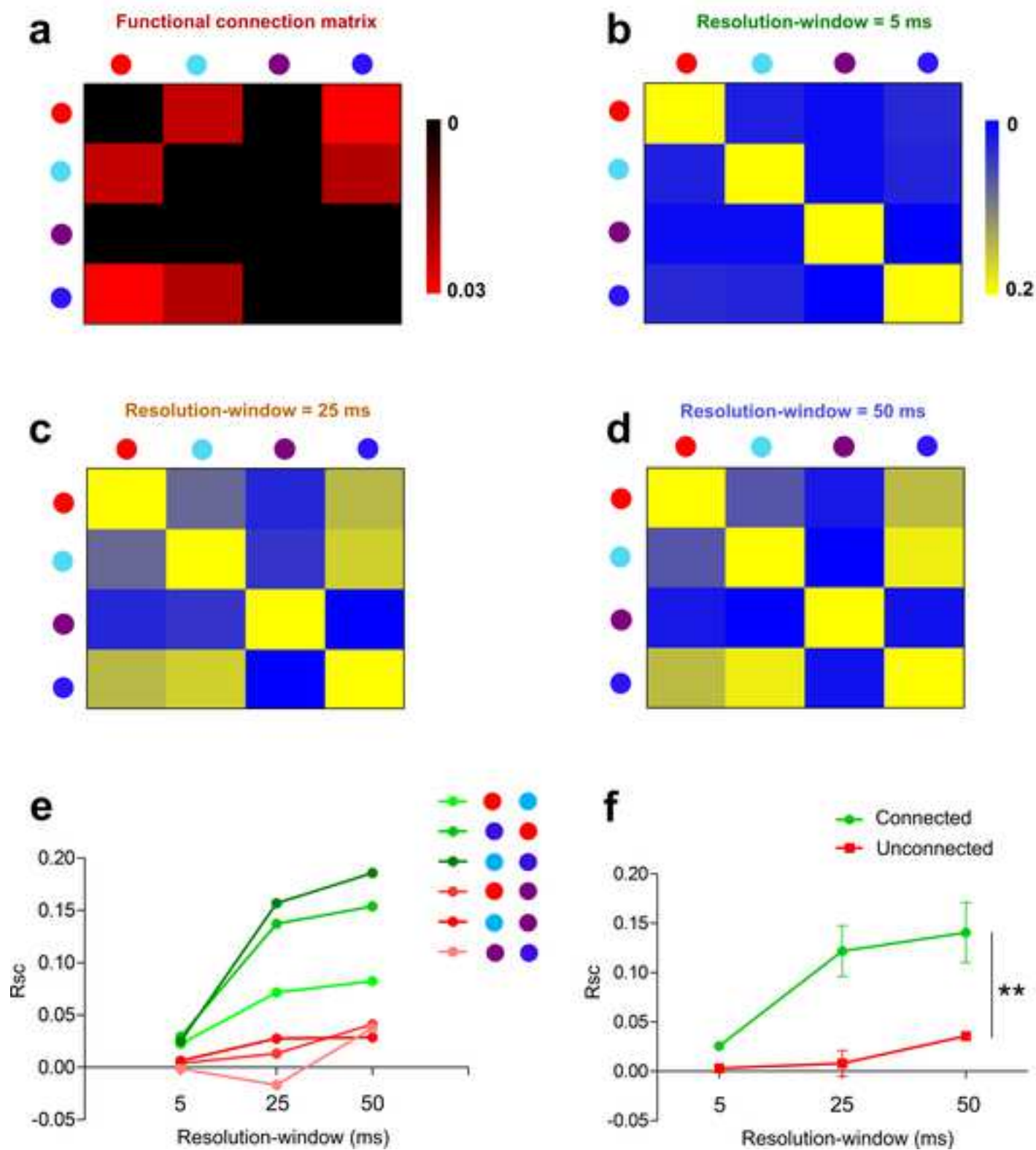
1
2
3
4
5
6
7
8
9
10
11
12
13
14
15
16
17
18
19
20
21
22
23
24
25
26
27
28
29
30
31
32
33
34
35
36
37
38
39
40
41
42
43
44
45
46
47
48
49
50
51
52
53
54
55
56
57
58
59
60
61
62
63
64
65

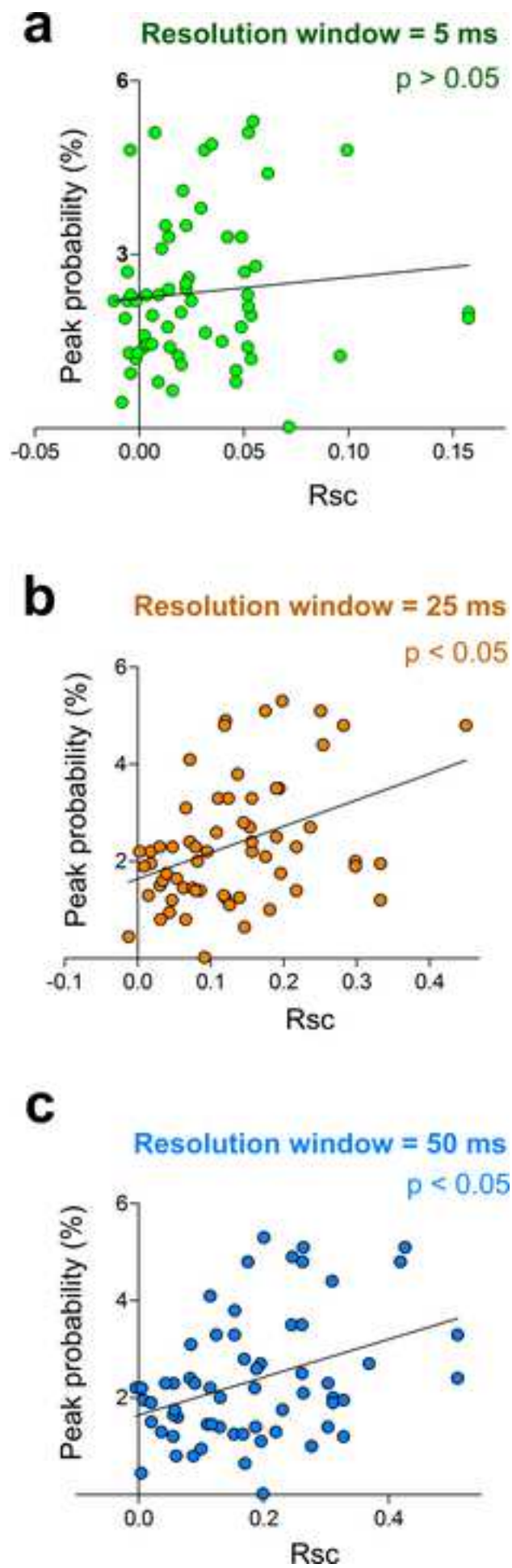
Tabular matrix representing the mean Rsc (red box stands for the connected pair, blue box corresponds to the unconnected pair) for every pair at every presented orientation. \bar{X} represents the mean.

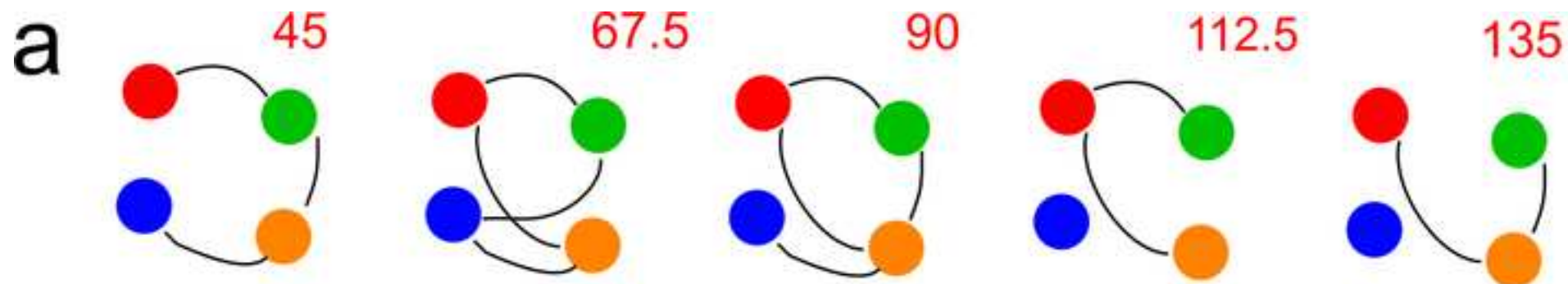
Fig. 6 Global trend for the functionally connected (green) and unconnected (red) pairs. Functionally connected neurons exhibited significantly higher noise correlation than the unconnected neuron pairs at all the resolution windows (Kolmogorov-Smirnov test, $p < 0.05$).











b

	45	67.5	90	112.5	135
	0.08	0.11	0.09	0.10	0.07
	0.14	0.11	0.11	0.17	0.07
	0.17	0.15	0.13	0.10	0.12
	0.14	0.15	0.04	0.08	0.12
	0.21	0.15	0.08	0.14	0.03
	0.15	0.14	0.13	0.09	0.17
<i>Connected \bar{X}</i>	0.17	0.14	0.11	0.14	0.15
<i>Unconnected \bar{X}</i>	0.13	0.12	0.06	0.10	0.07

Figure 6

